JOURNAL OF AIRCRAFT
Vol. 47, No. 3, May–June 2010

Computational-Fluid-Dynamics-Based Clean-Wing Aerodynamic Noise Model for Design

Serhat Hosder,* Joseph A. Schetz,† and William H. Mason‡
Virginia Polytechnic Institute and State University, Blacksburg, Virginia 24061-0203
Bernard Grossman§
National Institute of Aerospace, Hampton, Virginia 23666
and
Raphael T. Haftka¶
University of Florida, Gainesville, Florida 32611-6250

DOI: 10.2514/1.29105

A new noise metric is developed for clean-wing aerodynamic noise modeling that may be used in aircraft or wind turbine design studies involving aerodynamic noise. The method uses Reynolds-averaged Navier–Stokes calculations with a two-equation turbulence model to include the effects of the lift coefficient, flow three-dimensionality, and wing design parameters on the trailing-edge noise. These effects are not considered in the existing, relatively less expensive, semi-empirical noise prediction methods. The proposed noise metric is not the exact value of the noise intensity, but it is a relative noise measure suitable for design studies. The new noise metric is less expensive to compute compared to the full-noise calculations done with computational aeroacoustics methods, and it can be easily implemented using the solutions of Reynolds-averaged Navier–Stokes simulations that may have already been performed as part of the aerodynamic design and analysis. Parametric studies were performed to investigate the effect of the wing geometry and the lift coefficient on the noise metric. Two-dimensional studies were done using two subsonic (NACA 0012 and 0009) and two supercritical [SC(2)-0710 and -0714] airfoils. The energy-efficient transport wing (a generic conventional transport wing) was used for the three-dimensional study. Both two- and three-dimensional studies show that the trailing-edge noise increases significantly at high lift coefficients. The three-dimensional effects observed in the parametric wing study indicate the importance of calculating the noise metric with a characteristic velocity and length scale that vary along the span.

Introduction

AIRCRAFT noise has become an increasingly important design criterion and constraint in aircraft design in recent years. Although there has been a dramatic reduction in aircraft noise in the last three decades with the advances in engine and airframe technology, further reduction is still needed to minimize noise pollution, which requires addressing noise in the aircraft conceptual design. The present study introduces a new noise metric that may be used in aircraft or wind-turbine design studies involving clean-wing aerodynamic noise.

Airframe noise is defined as the *nonpropulsive* noise of an aircraft in flight [1]. Airframe noise sources on a conventional transport are the landing gear, trailing-edge flaps, leading-edge slats, the *clean* wing, and tail surfaces [2]. A clean wing has all its high-lift devices and the undercarriage in stowed position. The main noise mechanism of a clean wing is the trailing-edge (TE) noise. TE noise can be a significant contributor to the airframe noise for nonconventional configurations that do not use traditional high-lift devices on approach, such as a blended-wing–body aircraft with a large wing area and span or an airplane with a morphing wing. A TE-noise formulation based on proper physics may also be used to predict the noise originating from the trailing edges of flaps deflected with small angles that do not create significant flow separation. The TE noise of a conventional wing at high lift can be thought of as a *lower bound* value of the airframe noise on approach, as defined by Lockard and Lilley [3]. In other words, if the same lift required on approach can be obtained without using the traditional high-lift devices, the noise of the clean wing would be the lowest value that can be achieved for that particular aircraft as long as there is no massive separation on the wing. This value can be used as a measure of merit in noise-reduction studies.

With these facts as the motivation, and as the first step toward a general multidisciplinary design optimization noise model, the current study has focused on airframe noise modeling of a clean wing at approach conditions, which correspond to the position of an aircraft on a 3 deg glide slope, approximately 2000 m before touchdown at an altitude of 120 m. We investigate the effect of wing geometry (thickness ratio, t/c, and chord length, c) and the lift coefficient on the noise metric by performing two- and three-dimensional parametric studies.

The noise metric is a relative indicator of the clean-wing airframe noise suitable for design studies, but it is not necessarily the magnitude of the actual noise signature. Our methodology for obtaining the noise metric on a clean wing includes a modified version of the theoretical TE-noise-prediction models given in Goldstein [4] and Lilley [2,5]. We use 3-D, Reynolds-averaged Navier–Stokes (RANS) calculations with a two-equation turbulence model to obtain the characteristic velocity and length scales used in our model. The noise metric is less expensive to compute compared to the full-noise calculations done with computational aeroacoustics methods, and it can be easily implemented using the solutions of RANS simulations that may have already been performed as part of the aerodynamic design and analysis.

Received 30 November 2006; revision received 8 December 2009; accepted for publication 10 December 2009.

*Postdoctoral Associate; currently Assistant Professor of Aerospace Engineering, Missouri University of Science and Technology, Rolla, MO 65409. Senior Member AIAA.

†Fred D. Durham Endowed Chair, Department of Aerospace and Ocean Engineering. Fellow AIAA.

‡Professor, Aerospace and Ocean Engineering Department. Associate Fellow AIAA.

§Vice President, Education and Outreach. Fellow AIAA.

¶Distinguished Professor, Department of Aerospace Engineering, Mechanics and Engineering Science. Fellow AIAA.

Noise Metric

Clean-Wing Noise Modeling

TE noise comprises broadband and tonal components. The broadband component originates from the scattering of the acoustic waves generated due to the passage of the turbulent boundary layers over the trailing edge of wings or flaps [2]. The tonal component originates from the flow fluctuations created with vortices due to finite trailing-edge thickness. The noise metric presented in this study mainly models the broadband component, which is the dominant source for sharp trailing edges.

The broadband noise originating from the interaction of the turbulent flow along the surface with a sharp-edged body such as the trailing edge of a wing has been one of the main research areas of aeroacoustics for many years. Howe [6] gives a review of various TE-noise theories and lists them in different categories. Most of the theories used in predicting the TE noise are based on Lighthill's acoustic analogy [7]. Ffowcs Williams and Hall [8] were the first to solve the problem of noise radiated from the turbulent flow past a semi-infinite plate of zero thickness at zero angle of attack using this analogy. All theories on TE noise show that the noise intensity varies approximately with the fifth power of the freestream velocity [1,6]. It is also proportional to the trailing-edge length along the span and a characteristic length scale for turbulence.

Most of the TE-noise-prediction methods [9,10] used today are based on semi-empirical methods. In these methods, characteristic length and velocity scales are usually determined using simplified assumptions, and the formulations are calibrated with experimental data or flight measurements. One such method is the Aircraft Noise Prediction Program [11] (ANOPP), which is widely used in design studies that involve aircraft noise. In the ANOPP clean-wing noise module, the TE-noise prediction is formulated for a range of low lift coefficient values. Within this range, the characteristic length and velocity scales used in the model, and thus the clean-wing noise prediction, are independent of the change in the lift coefficient. However, the increase in TE noise can be significant at high lift coefficients, as will be shown in our two- and three-dimensional parametric studies, which include the comparison of noise predictions from ANOPP to the predictions of the new noise metric developed here. We will also include the predictions from a recent clean aircraft noise formulation of Lockard and Lilley [3] in some of our parametric studies. Lockard and Lilley [3] used this formula to approximate the far-field noise intensity from a clean wing at high lift. The method of Lockard and Lilley and our model have common points in their derivation, and both methods take into account the change of TE noise with the lift coefficient. However, the method by Lockard and Lilley used the results of two-dimensional RANS calculations on a generic airfoil to model the variation of the noise intensity as a function of the lift coefficient, whereas we perform 3-D RANS calculations for each specific geometry of interest and take into account the spanwise variation of the velocity and length scales, which become important at high lift coefficients for three-dimensional cases.

In recent years, computational aeroacoustics methods [12] have been used to simulate acoustic scattering from trailing edges. These methods couple time-accurate flowfield data obtained from RANS or large eddy simulation solutions with acoustic equations to propagate the noise to the far field. They can give accurate results; however, they are restricted to simple problems due to the very high computational expense stemming from the very fine time- and space-resolution requirements. Considering the complexity of typical geometries and the number of runs required in design studies that include aerodynamic noise, it will be impractical to use computational aeroacoustics in design.

Formulation of the Noise Metric

Both the experimental and computational aeroacoustics studies verify the relevance of modeling the turbulent boundary-layer–trailing-edge (TBL-TE) noise created over the sharp trailing edges of airfoils and wings to the theoretical analysis of the half-plane scattering problem studied by Ffowcs Williams and Hall. Therefore, in the derivation of the new noise metric, the results obtained from Ffowcs Williams and Hall become the starting point. The originality of the current noise metric is in the modeling of the characteristic velocity and length scales in a way suitable for design studies while capturing the important physics of the problem.

Following the approach of Goldstein [4], one can approximate the far-field noise intensity per unit volume of acoustic sources at the trailing edge of a wing as

$$I \approx \frac{\rho_\infty}{2\pi^3 a_\infty^2 H^2}\omega_0 u_0^4 \tag{1}$$

where ρ_∞ is the freestream density, a_∞ is the freestream speed of sound, ω_0 is the characteristic source frequency, u_0 is the characteristic velocity scale for turbulence, and H is the distance to the ground (receiver). This equation is a form of the Ffowcs Williams and Hall equation given by Goldstein [4]. It is also similar to the form given in Howe [6,13] and Crighton [1]. Equation (1) gives the noise intensity at a point in the flyover plane where the polar angle (θ) is 90 deg, and it is written for a trailing-edge sweep angle (β) of zero. Therefore, it does not show the dependency of the noise intensity on the directivity and the trailing-edge sweep angles. Following the approach given in Howe [6], the trailing-edge sweep-angle dependency can be included by multiplying Eq. (1) with the term $\cos^3\beta$:

$$I \approx \frac{\rho_\infty}{2\pi^3 a_\infty^2 H^2}\omega_0 u_0^4 \cos^3\beta \tag{2}$$

To write the noise intensity for any point in the far field, a directivity term, $D(\theta, \psi)$, may be included in the Eq. (2) to give

$$I \approx \frac{\rho_\infty}{2\pi^3 a_\infty^2}\omega_0 u_0^4 \cos^3\beta \frac{D(\theta,\psi)}{H^2} \tag{3}$$

Here, the directivity term is in the form given by Ffowcs Williams and Hall [8]:

$$D(\theta,\psi) = 2\sin^2\left(\frac{\theta}{2}\right)\sin\psi \tag{4}$$

where θ is the polar directivity angle and ψ is the azimuthal directivity angle. (Fig. 1).

The Doppler factors due to convection of acoustic sources are not included in Eq. (3), because the focus of the current study is on flows with low Mach numbers that are between 0.2 and 0.3 for typical aircraft at approach before landing. As indicated by Lilley [2] and Lockard and Lilley [3], the equivalent noise sources in the wing boundary layer are in motion relative to the wing; therefore, they

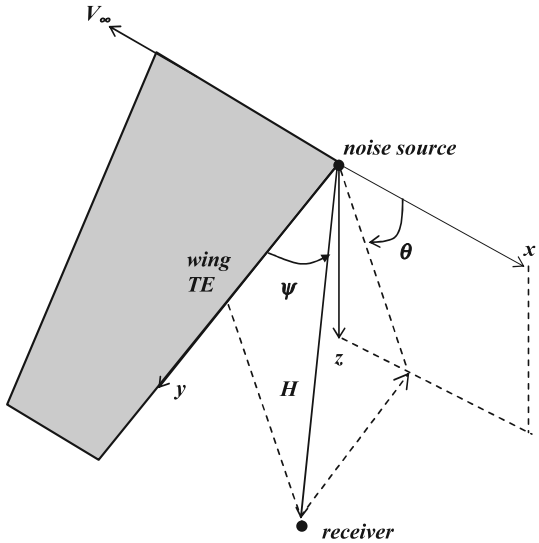

Fig. 1 Directivity angles used in the noise metric. Note that the trailing-edge sweep angle (β) is 0 deg here.

appear to be moving very slowly to an observer on the ground. The relative velocity between the sources and the observer determines the magnitude of the Doppler factors. Because the relative velocity is small for the cases considered in this study, the Doppler factors may be omitted.

Using the Strouhal relation for turbulent flow [2],

$$\frac{w_0 l_0}{u_0} \approx \text{const} \tag{5}$$

one can rewrite Eq. (3) with the characteristic length scale for turbulence l_0:

$$I \approx \frac{\rho_\infty}{2\pi^3 a_\infty^2} u_0^5 l_0^{-1} \cos^3\beta \frac{D(\theta,\psi)}{H^2} \tag{6}$$

Because it is desirable to design a wing for minimum noise, one should consider the spanwise variation of the characteristic velocity, characteristic length scale, the trailing-edge sweep, and the directivity angles (i.e., $u_0 = u_0(y)$, $l_0 = l_0(y)$, $\beta = \beta(y)$, $\theta = \theta(y)$, and $\psi = \psi(y)$). Because the changes in the characteristic velocity and length scale are significant along the span at higher lift coefficients, the importance of retaining the spanwise variation of these variables will be shown with the three-dimensional parametric studies. Assuming a correlation volume per unit span at the trailing edge as

$$\mathrm{d}V = l_0^2 \,\mathrm{d}y \tag{7}$$

Equation (6) can be written for the correlation volume given in Eq. (7) and integrated over the span b to obtain

$$I_{\mathrm{NM}} = \frac{\rho_\infty}{2\pi^3 a_\infty^2} \int_0^b u_0^5 l_0 \cos^3\beta \frac{D(\theta,\psi)}{H^2} \,\mathrm{d}y \tag{8}$$

where I_{NM} is a noise-intensity indicator that can be evaluated on the upper or the lower surface of the wing. Note that I_{NM} is not the exact value of noise intensity; however, it is expected to be an accurate indicator as a relative noise measure. The noise-intensity indicator I_{NM} is scaled with the reference noise intensity of 10^{-12} W/m^2 (i.e, the minimum sound intensity level that a human ear can detect, which is a common practice in acoustics). Finally, the proposed noise metric (NM) for the TE noise (in decibels) can be written as

$$\mathrm{NM} = 120 + 10\log(I_{\mathrm{NM}}) \tag{9}$$

To obtain the total noise metric for a wing, the noise-metric values are calculated for the upper ($\mathrm{NM}_{\mathrm{upper}}$) and the lower surfaces ($\mathrm{NM}_{\mathrm{lower}}$), and added as

$$\mathrm{NM} = 10\log(10^{\frac{\mathrm{NM}_{\mathrm{upper}}}{10}} + 10^{\frac{\mathrm{NM}_{\mathrm{lower}}}{10}}) \tag{10}$$

Modeling of u_0 and l_0

In the new noise metric, the characteristic turbulent velocity at a spanwise location of the wing trailing edge can be chosen as the maximum value of the turbulent kinetic energy (TKE) profile at that particular spanwise station:

$$u_0(y) = \mathrm{Max}[\sqrt{\mathrm{TKE}(z_n)}] \tag{11}$$

Here, z_n is the direction normal to the wing surface. Others have proposed the same choice for the characteristic velocity in their noise models [3]. It is proposed here that the characteristic turbulence length scale for each spanwise station can be well represented by

$$l_0(y) = \frac{\mathrm{Max}[\sqrt{\mathrm{TKE}(z_n)}]}{\omega} \tag{12}$$

where ω is the turbulence frequency (dissipation rate per unit kinetic energy) observed at the maximum TKE location. This choice of a length scale is directly related to the turbulent characteristics of the flow and is indicative of the size of the turbulent eddies that produce the noise. It can be viewed as more soundly based than other suggestions in the literature such as the boundary-layer thickness or the displacement thickness. Those lengths are related to the mean flow and not connected directly to the turbulence structure. The TKE and the turbulence frequency (ω) are obtained from the solutions of the TKE–ω (k–ω) turbulence model equations used in the RANS calculations.

Computational Fluid Dynamics Simulations

The computational fluid dynamics (CFD) code GASP [14] has been used for physical modeling of all validation and parametric noise-metric cases presented in this paper. GASP is a three-dimensional, structured, multiblock, finite volume, RANS code. In the CFD simulations, inviscid fluxes were calculated by an upwind-biased third-order spatially accurate Roe flux scheme. Asymptotic convergence to a steady-state solution was obtained for each case. The iterative convergence of each solution was examined by monitoring the overall residual, which is the sum (over all the cells in the computational domain) of the L^2 norm of all the governing equations solved in each cell. In addition to this overall residual information, some of the output quantities such as the lift coefficient and the TKE distributions were also monitored. Grid sequencing was used to reduce the number of iterations required to converge to a steady-state solution. In the CFD simulations, we solved full Navier–Stokes equations by including all the viscous terms in the physical model. All the runs were made with the assumption of fully turbulent flow. Menter's k–ω shear stress transport turbulence model [15] was used in all the calculations. This model has been shown [16] to give better overall accuracy in different types of flows compared to the other two-equation turbulence models.

Noise-Metric Validation

Noise-metric validation was performed with the seven test cases, shown in Table 1. These cases were selected from a two-dimensional NACA 0012 experimental database. To create this database, Brooks et al. [10] conducted experiments at different speeds, angles of attack, and chord lengths using NACA 0012 airfoils and measured the one-third octave sound pressure level (SPL) spectra of the noise generated by the airfoils. They also used this database to develop a semi-empirical airfoil self-noise prediction method. The SPL spectrum of each case was measured at a point 1.22 m away from the midspan trailing edge. Both directivity angles θ and ψ were 90 deg at this location. The main noise mechanism of all the cases used in the validation study is the TE noise generated by the scattering of turbulent pressure fluctuations over the trailing edge (see Table 1). These cases were chosen to cover a wide range of speeds at different angles of attack.

CFD simulations were performed for each noise-metric-validation case. The noise metric of each case, NM_i, was calculated using the characteristic velocity and the length scales obtained from the CFD simulations in Eq. (10) with Eqs. (11) and (12). For the same cases, the overall sound pressure levels (OASPL_i) were calculated from the experimental data. The noise metric for each case was scaled with the value obtained for case 1 using the following equation:

$$\overline{\mathrm{NM}_{si}} = 10^{[0.1(\mathrm{NM}_i - \mathrm{NM}_1)]} \tag{13}$$

Table 1 Experimental NACA 0012 airfoil test cases used in the noise-metric validation

Case (i)	α, deg	Chord length, m	V_∞	Mach	$Re_c \times 10^{-6}$
1	0.00	0.3048	71.3	0.208	1.497
2	0.00	0.3048	31.7	0.092	0.665
3	2.00	0.2286	31.7	0.092	0.499
4	1.50	0.3048	39.6	0.116	0.831
5	0.00	0.3048	55.5	0.162	1.164
6	2.00	0.2286	71.3	0.208	1.122
7	1.50	0.3048	71.3	0.208	1.497

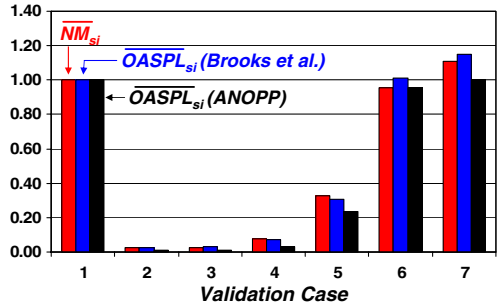

Fig. 2 Comparison of $\overline{\mathrm{NM}}_{si}$ and the $\overline{\mathrm{OASPL}}_{si}$ values obtained with ANOPP to the experimental $\overline{\mathrm{OASPL}}_{si}$ values of Brooks et al. [10] for each NACA 0012 validation case.

A similar scaling was done for the OASPL values:

$$\overline{\mathrm{OASPL}}_{si} = 10^{[0.1(\mathrm{OASPL}_i - \mathrm{OASPL}_1)]} \tag{14}$$

Figure 2 shows the comparison of NM_{si} and OASPL_{si} for each case. As can be seen from this figure, the agreement in trends between the experiment and our predictions are good at various speeds and angles of attack. This figure also demonstrates that the noise metric is capable of capturing the variations in the TE noise as a relative noise measure when different flow conditions and parameters are changed. Figure 2 also shows the noise predictions obtained with ANOPP [11]. For relative comparison, the OASPL predictions from ANOPP are scaled with the reference value obtained for case 1 and presented for the $\overline{\mathrm{OASPL}}_{si}$ variable, which is calculated with Eq. (14). For all validation cases, the relative change in the noise metric is closer to the change in experimental OASPL values than the ANOPP predictions.

Although the cases presented here provide valuable results for the validation of the noise metric, comparison with three-dimensional experimental data obtained for the TE-noise intensity of a clean wing at approach speeds and Reynolds numbers should be performed in future studies for a more comprehensive validation of the noise metric, which will also enhance the reliability of its use.

Parametric Noise-Metric Studies

The influence of the flight speed on the TE noise is well known through the fifth power of the velocity, as shown by all the aeroacoustic theories on the subject. This effect is included in the proposed noise metric, because the characteristic velocity u_0 will change as the freestream velocity changes. The noise metric also includes some parameters explicitly in the model, such as the directivity angles θ and ψ, the distance to the observer H, and the trailing-edge sweep β. The functional dependency of TE noise on these variables are again well described by the trailing-edge theories [6,8]. However, in addition to the speed and other explicit parameters, one also would like to know the effect of the other variables used in aerodynamic optimization problems such as the lift coefficient and the wing geometry (thickness, airfoil shape, twist, etc.). The information obtained from parametric studies provides valuable information about the effect of these variables on the TE noise as predicted by the new noise metric. The parametric studies include both two- and three-dimensional cases. Two-dimensional parametric studies were done using two symmetric NACA four-digit airfoils (NACA 0012 and 0009) and two supercritical (SC(2)-0710 and -0714) airfoils. A generic conventional transport wing was used for the three-dimensional studies.

Two-Dimensional Studies

NACA 0009 and 0012 Airfoils

The main purpose of the study with NACA 0012 and 0009 airfoils was to investigate the noise change due to the lift coefficient and the thickness ratio. To meet this objective, the lift coefficient was reduced while increasing the chord length to have the same lift at a constant speed. Further reduction was sought by decreasing the thickness ratio. This 2-D study can be thought of as a simplified representation of increasing the wing area and reducing the overall lift coefficient of an aircraft at constant lift and speed.

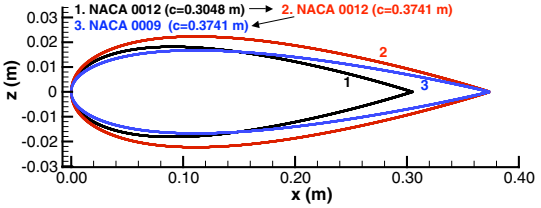

Fig. 3 NACA 0012 and 0009 airfoils with different chord lengths used in the noise reduction study.

Three configurations were considered (Fig. 3): 1) NACA 0012 airfoil with a chord length of 0.3048 m at $\alpha = 10$ deg, 2) NACA 0012 airfoil with a chord length of 0.3741 m $\alpha = 8$ deg, and 3) NACA 0009 airfoil with a chord length of 0.3741 m $\alpha = 8$ deg. All cases were run with a freestream velocity (V_∞) of 71.3 m/s and a Mach number of 0.2. The Reynolds number based on the chord (Re_c) was 1.497×10^6 for case 1 and 1.837×10^6 for the other two cases. Both Reynolds numbers are large enough to be able to model the flow as fully turbulent. The airfoil geometries and flow conditions are similar to those used in the validation studies. CFD simulations were performed for each case. Computational grids had C topologies, each with 388 cell centers in the streamwise direction and 64 points in the normal direction to the airfoil surface. The noise metric was calculated at a distance (H) 1.22 m away from the trailing edge with the directivity angles of $\theta = 90$ deg and $\psi = 90$ deg (the same values used in the validation studies). Note that these values are arbitrary because we are interested in the relative change of the noise metric and we assume that the receiver is at the same location for all the cases.

Figure 4 shows the noise-reduction history of this study. We started with case 1 with the NACA 0012 airfoil at a lift coefficient (C_l) of 1.046. C_l was reduced to 0.853 for case 2 while increasing the chord length by 23% to keep the lift at a constant value of approximately 1010 N. A noise reduction of 2.45 dB was achieved between cases 1 and 2. When the thickness of the airfoil was decreased by 25% (NACA 0009) while keeping the same chord length and lift, an additional reduction of 1.16 dB in the noise metric was observed. The total noise reduction was 3.61 dB . Decreasing the lift coefficient contributed 68% of the total noise reduction. This example shows that it is possible to reduce the TE noise by increasing the chord length (wing area) and decreasing the lift coefficient and the thickness ratio.

SC(2)-0710 and -0714 Airfoils

In addition to the NACA four-digit airfoil cases, two-dimensional parametric studies were performed with supercritical airfoils at realistic flight conditions to study the effect of the lift coefficient and the thickness ratio on the noise metric. We used two supercritical airfoils, SC(2)-0710 and -0714 (Fig. 5), that are similar to the supercritical wing sections used in modern transport aircraft. These airfoils belong to the same family, but have different thickness ratios

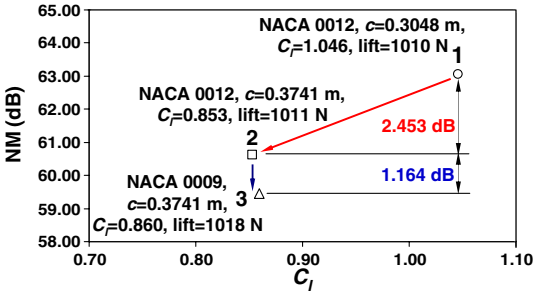

Fig. 4 Noise-metric-reduction history obtained with NACA 0012 and 0009 airfoils for various lift coefficients at constant lift.

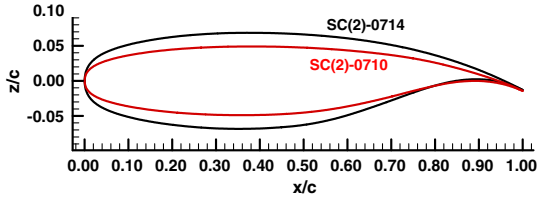

Fig. 5 SC(2)-0710 and -0714 airfoils.

[17] ($t/c = 10\%$ for SC(2)-0710 and $t/c = 14\%$ for SC(2)-0714). The thicker airfoil can be thought of as a representative inboard wing section, whereas the thinner one can be an example airfoil at an outboard station of a typical transport wing. CFD simulations were performed at $Re_c = 44 \times 10^6$ with $V_\infty = 68$ m/s and Mach = 0.2. These values approximately correspond to the conditions of a typical transport aircraft with a mean aerodynamic chord of 9.54 m at an altitude of 120 m before landing. At this location, the aircraft is approximately above the point where the noise certification measurements at approach are taken. Airfoil grids used in the CFD calculations had 388×64 cells. The noise-metric values were calculated for $H = 120$ m, $\theta = 90$ deg, and $\psi = 90$ deg.

For each airfoil, the angle of attack was increased to get the highest lift coefficient before stall. The drag polar of each airfoil is shown in Fig. 6. As can be seen in this figure, SC(2)-0710, the airfoil with the smaller thickness ratio, has a lower maximum section lift coefficient value compared to the SC(2)-0714 airfoil. For lift coefficients greater than 0.8, the drag of the SC(2)-0710 airfoil is larger at the same lift.

Looking at the noise-metric values (Fig. 7), we see that the noise of each airfoil stays approximately constant up to a certain lift coefficient value. At this range of lower C_l, the thicker airfoil has higher noise-metric values. The difference is approximately 2 dB at $C_l = 0.7$. A dramatic increase in the noise-metric value can be observed for each airfoil at higher lift coefficients. The large increase in the noise metric at high lift coefficients originates from the increase of both the maximum TKE and the characteristic length scale l_0. Figure 8 shows the TKE and the length-scale profiles at the upper surface trailing edge of both airfoils for different lift coefficients. The significant increase in the maximum TKE values can be seen at higher lift coefficient values. A similar observation can be made for the length scale. At high lift coefficients, the adverse pressure gradient close to the upper surface trailing edge increases the thickness of the turbulent boundary layer and the magnitude of the turbulent fluctuations. These values become larger as the flow gets closer to separation. A detailed analysis of the behavior of the characteristic velocity and the length scales can be found in Hosder [18].

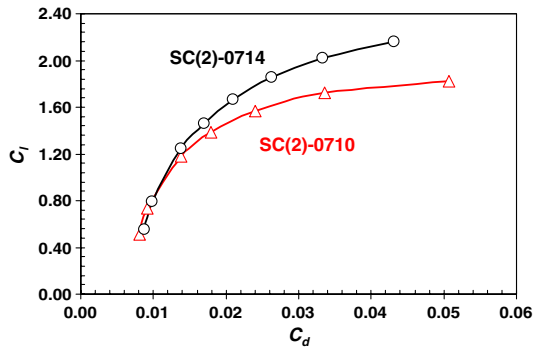

Fig. 6 Drag polars for the SC(2)-0710 and -0714 airfoils.

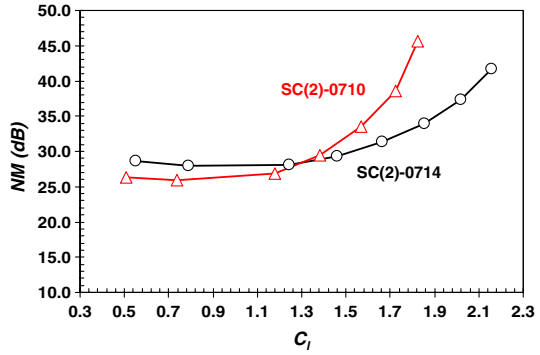

Fig. 7 Comparison of total noise-metric values obtained with the SC (2)-0710 and -0714 airfoils.

Figure 9 gives a comparison of the noise-metric results of the SC (2)-0714 airfoil and the OASPL values predicted with the formula derived by Lockard and Lilley [3]. The predictions obtained with ANOPP [11] are also included to emphasize the fact that OASPL values calculated with this method do not change with the lift coefficient. Both the new noise metric and the OASPL values are scaled with their corresponding values at $C_L = 0.550$ so that a comparison of the relative change can be made. As can be seen from this figure, both the noise metric and the approximation by Lockard and Lilley capture the increase in noise as C_l increases. However, there are differences in the actual values at each lift coefficient, which may be due the different airfoil geometry (NACA 4412) used in the derivation of Lockard and Lilley's model.

Three-Dimensional Study

The objective of the three-dimensional study was to examine the effect of the overall lift coefficient C_L on the clean-wing airframe noise by using a realistic wing geometry at approach conditions. This study also permitted an investigation of the spanwise variation of the characteristic velocity and length scale as the lift coefficient was changed.

The geometry used in this study is the energy-efficient transport (EET) wing [19]. This is a generic conventional transport aircraft wing (Fig. 10a) used in many experimental studies at NASA. For our study, we scaled the original dimensions of the experimental model so that the mean aerodynamic chord is 9.54 m. The scaled wing has a reference area (S_{ref}) of 511 m^2 and a span of 64.4 m. Note that the planform area includes the leading- and trailing-edge extensions in the inboard section. Unless specified with a subscript, all lift and drag coefficients (C_L and C_D) presented in this study use S_{ref} for scaling. The trapezoidal wing area, which does not include the leading- and trailing-edge extensions in the inboard section, is 83% of the planform area. The wing has an aspect ratio of 8.16, a dihedral angle of 5 deg, and a sweep angle of 30 deg at the quarter chord. The outboard section of the wing starts at $2y/b = 0.375$. Wing sections are supercritical airfoils with $t/c = 14\%$ at the root, $t/c = 12\%$ at the break point, and $t/c = 10\%$ at the tip. These geometric parameters and flow conditions ($Re_{\text{mac}} = 44 \times 10^6$, $V_\infty = 68$ m/s, and Mach = 0.2) correspond to the approach conditions of a typical large transport aircraft . The computational grid used in the CFD simulations has a C-O topology consisting of four blocks with a total number of 884,736 cells (Figs. 10a and 10b). We evaluate the noise metric at an altitude of 120 m for an observer at the ground level directly below the aircraft, which corresponds to $\theta = 90$ deg at $y = 0$ plane (see Fig. 1). The azimuthal angle ψ is calculated at each spanwise station; however, the effect of the change in ψ along the span is negligible.

EET wing calculations were performed at eight different angles of attack ranging from 0 to 14 deg in increments of 2 deg. Figure 11a shows the lift coefficients and corresponding wing loading (W/S) values with the assumption of straight and level flight (lift equal to the weight of the airplane) for an airplane obtained at each angle of attack. The C_L vs α curve is linear up to 12 deg, where $C_L = 1.084$. At the last angle of attack, one can see the break of the linear variation, which indicates stall. This can also be seen from the drag polar given in Fig. 11b. The sharp increase in drag at the last angle of attack, where $C_L = 1.106$, is due to a large flow separation on the wing. With this wing configuration, the highest wing loading value that could be achieved was 315.7 kg/m^2 (64.8 lb/ft^2). On the other hand, for a B-777 type of transport aircraft, we find that W/S is approximately 432 kg/m^2 (88.8 lb/ft^2) when using the maximum

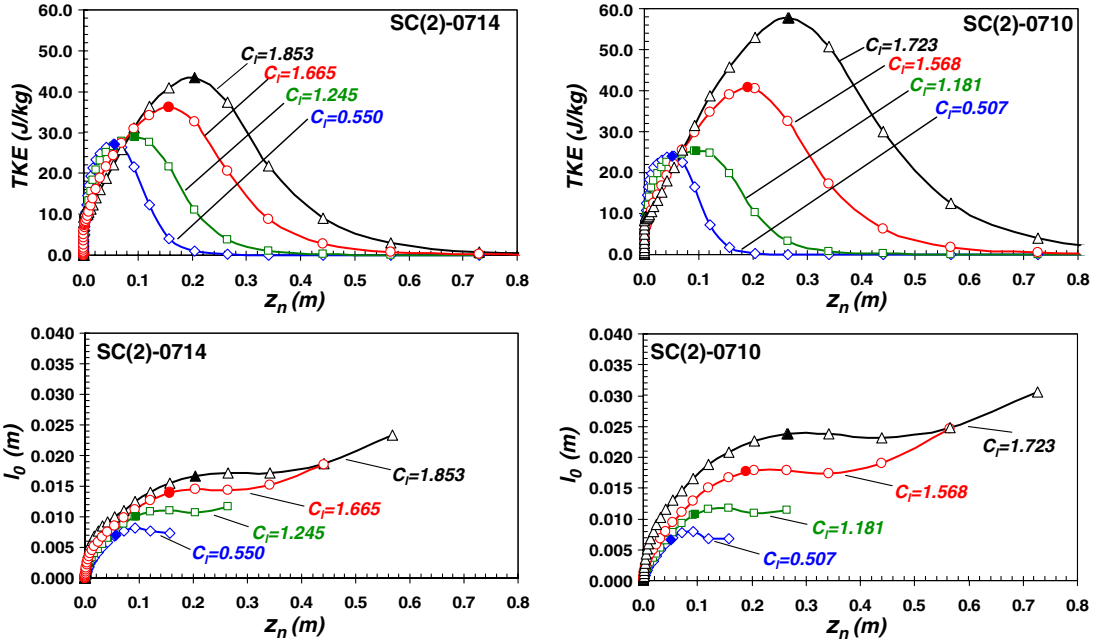

Fig. 8 TKE and l_0 profiles at the upper surface trailing edge of the SC(2)-0710 and -0714 airfoils for various section lift coefficients. The filled symbols show the maximum TKE and corresponding length-scale values.

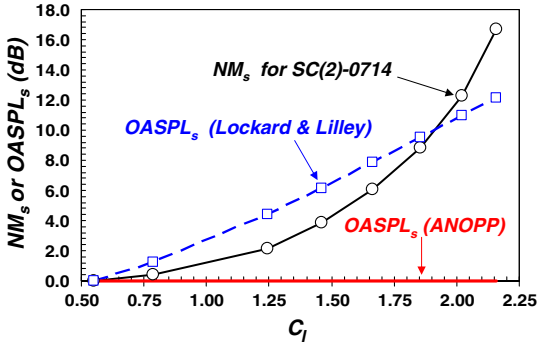

Fig. 9 Comparison of the scaled NM_s of the SC(2)-0714 airfoil, and the scaled $OASPL_s$ obtained with the method by Lockard and Lilley [3] and ANOPP [11].

design landing weight of such an aircraft and the S_{ref} of our wing. Although one can reach relatively high lift coefficients with a clean wing by increasing the angle of attack without having substantial separation, it is clear that it would be almost impossible to achieve the lift required to sustain a conventional aircraft at the approach without using high-lift devices.

The section lift coefficient (C_l) and the span-load distributions are given in Figs. 12a and 12b. The span load and C_l exhibit smooth variations along the half-span for all C_L except the highest value. At this lift coefficient, a large loss in lift on the outboard section of the wing starting from $2y/b \approx 0.6$ can be seen. Figure 13 shows the skin-friction (C_f) contours of the wing upper surface at two lift coefficients. The skin-friction values presented in this figure were obtained using the component of the wall shear stress in the freestream direction on each cell face of the wing upper surface [14]. For $C_L = 0.375$, the skin-friction lines show a smooth pattern along the span except for the small kink at the break point. For $C_L > 0.970$, the skin friction drops to negative values at the trailing edge of the outboard wing, indicating incipient flow separation. Although the incipient flow separation that occurs very close to the trailing edge does not have a significant effect on the lift characteristics and general pressure field on the wing, its influence on the TE noise may be important, because the change in the maximum TKE and the characteristic length scale become significant when the flow is close to separation, as seen in the two-dimensional studies. It should be noted that the TE-noise metric may not be accurate for massively

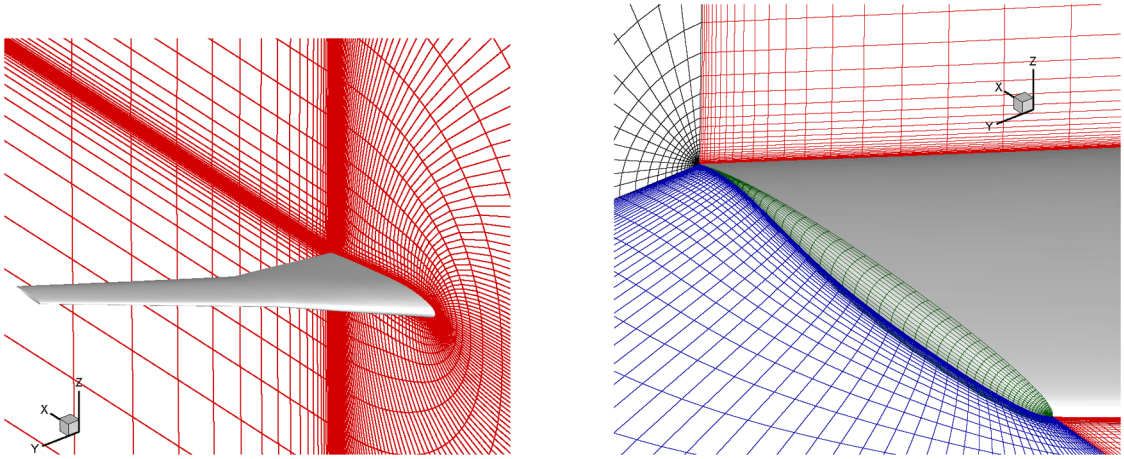

a) The C grid around the root section **b) A view of the grid in the tip region**

Fig. 10 EET wing and the grid used in the 3-D parametric studies

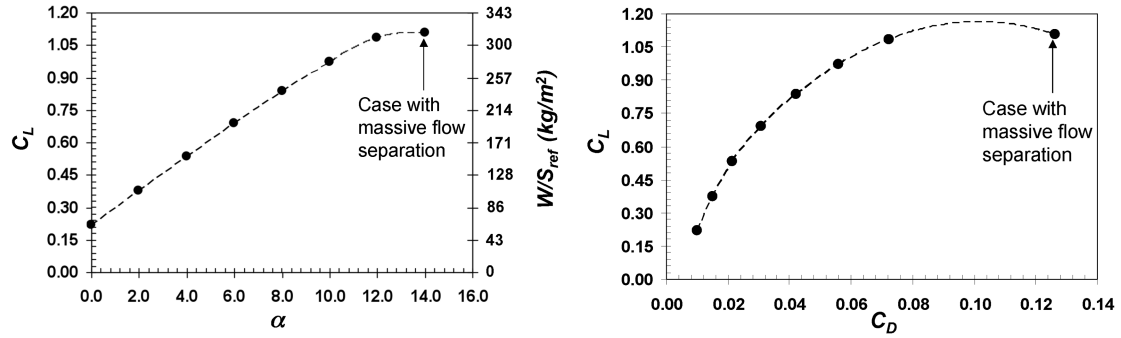

a) C_L and W/S vs. (α) b) Drag polar

Fig. 11 Lift and drag characteristics of the EET wing

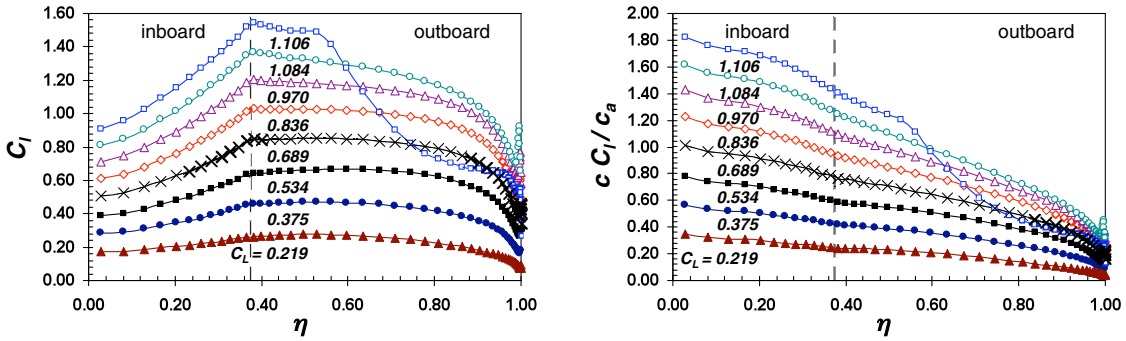

a) Section lift coefficient b) Span load

Fig. 12 Section lift coefficient and span-load distributions of the EET wing

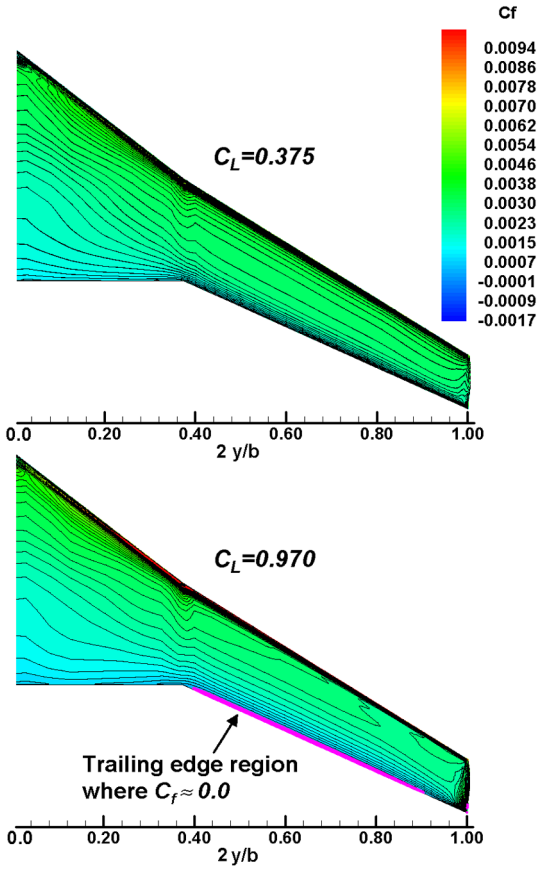

Fig. 13 Skin-friction contours on the upper surface of the EET wing at two C_L values.

separated flows (i.e., the case with $\alpha = 14$ deg and $C_L = 1.106$ in the current study) due to the assumptions made in the acoustic theory used in its derivation and the difficulty in predicting the TKE and the length scales with steady RANS models for such flows. Therefore, we excluded that case from our noise-metric results.

Looking at the maximum TKE (Fig. 14a) and the characteristic length-scale (Fig. 14b) distributions along the span, we see that the change in these quantities is small along the span at lower lift coefficients ($C_L < 0.836$), except for the tip region where we see the effect of the tip vortex and an increase in TKE. The tip vortex region is small at moderate angles of attack and does not have a significant effect on the overall noise metric [18]. The three-dimensional effects become important at higher lift coefficients ($C_L \geq 0.836$). One can see a significant increase in TKE_{max} and l_0 starting from $C_L = 0.836$, especially on the outboard section of the wing where the section lift coefficients are higher. Because the section lift coefficients remain at relatively low values in the inboard section, the change in the TKE and length scale is not as large as the one observed for the outboard section. These results are consistent with the earlier observations made about the skin-friction change on the upper surface of the wing. The skin-friction values approaching zero at the trailing edge of the outer wing imply the increase in TKE_{max} and the length scale. At $C_L = 1.084$, which corresponds to $\alpha = 12$ deg, a large separation region is not observed, but incipient flow separation at the trailing edge of the outboard wing can still cause a significant increase in TKE_{max} and l_0.

At higher lift coefficient values, the maximum TKE and l_0 are not uniform along the span, and they get larger at the outboard sections due to three-dimensional effects. This shows the importance of calculating the noise metric, especially at high lift coefficients, with a characteristic velocity and length scale that vary along the span. It also points to the fact that using an average value for the characteristic velocity or the length scale along the span will not work at higher lift coefficients, simply because the noise metric is proportional to the integration of the $u_0^5 \times l_0$ term along the span and $\bar{u}_0^5 \times \bar{l}_0$ is not equal to $\bar{u}_0^5 \times \bar{l}_0$ in general (here, the overbar is used to represent the average along the span).

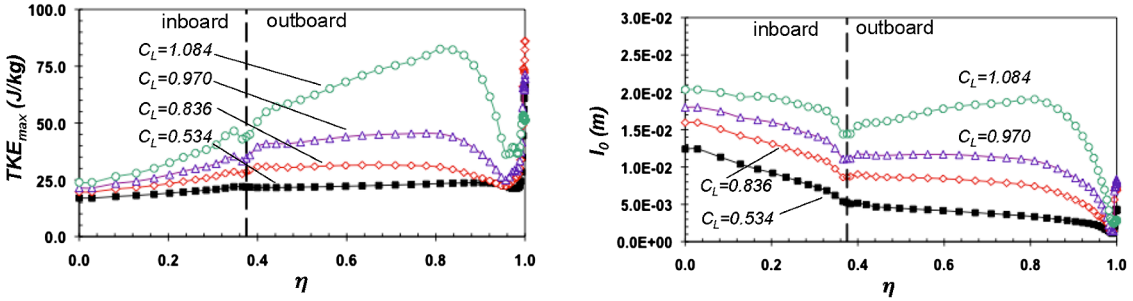

a) Maximum TKE b) Characteristic length scale (l_0)

Fig. 14 Distributions along the upper surface trailing edge of the EET wing

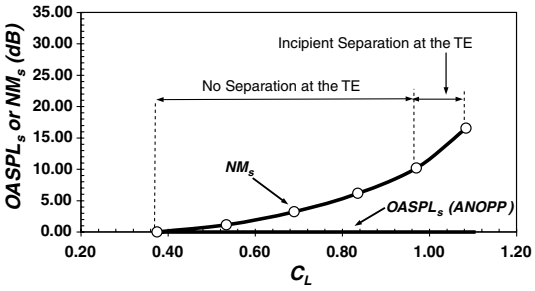

Fig. 15 Comparison between the scaled NM_s and the scaled $OASPL_s$ obtained with ANOPP [11]. The noise-metric results and the OASPL values are scaled with their corresponding values at $C_L = 0.375$.

The noise-metric results for the EET wing are given in Fig. 15. At lower lift coefficient values ($C_L \leq 0.534$), the noise metric remains approximately constant. When C_L exceeds 0.534, a gradual increase in the noise metric can be noticed. At $C_L = 0.970$, the noise metric becomes 6.6 dB higher than the value obtained at $C_L = 0.534$. Note that, in the skin-friction results for $C_L \leq 0.970$, no flow separation was observed on the upper surface of the wing. However, for $0.970 < C_L < 1.106$, mild separation at the trailing edge of the outboard wing was detected. For this range of C_L, a larger increase in the noise can be seen. The change in the TE noise becomes 12.7 dB between $C_L = 0.375$ and 1.084. The OASPL values obtained with ANOPP remains constant with the lift coefficient, as observed for the two-dimensional cases.

Conclusions

A new noise metric was developed that may be used in optimization problems that involve aerodynamic noise from any clean-wing geometry, including wind-turbine blades. The noise metric is a relative indicator of the clean-wing airframe noise suitable for design studies, but it is not necessarily the magnitude of the actual noise signature. The proposed model includes characteristic velocity and length scales that are obtained from three-dimensional, steady, RANS simulations with a two-equation k–ω turbulence model and is capable of capturing three-dimensional effects that become important at high lift coefficients. The new noise metric can also capture the effects of different design variables on the clean-wing airframe noise, such as the aircraft speed, lift coefficient, and wing geometry. Compared to the full-noise calculations done with computational aeroacoustics methods, the noise metric is much less expensive to compute and can be easily obtained using the solutions of RANS simulations that may have already been performed as part of the aerodynamic design and analysis.

Parametric studies were performed to investigate the effect of different design variables (wing geometry and lift coefficient) on the noise as indicated by the noise metric. Two-dimensional parametric studies were done using two subsonic (NACA 0012 and 0009) and two supercritical (SC(2)-0710 and -0714) airfoils. The EET wing (a generic conventional transport wing) was used for the three-dimensional study.

The two-dimensional studies showed that the large increase in the noise metric at high lift coefficients originates from the increase of both the maximum TKE and the length scale at the trailing edge of the suction side. An example study with the NACA 0012 and 0009 airfoils demonstrated a reduction in the TE noise by decreasing the thickness ratio and the lift coefficient, while increasing the chord length to keep the same lift at a constant speed. This 2-D study can be considered a simplified representation of increasing the wing area and reducing the overall lift coefficient of an aircraft at constant lift and speed.

Both two- and three-dimensional studies demonstrated that the TE noise remains almost constant at low lift coefficients ($C_L < 0.6$), whereas it gets larger at higher lift coefficients. The EET wing study also showed that, at higher lift coefficient values, the maximum TKE and l_0 are not uniform along the span, and they get larger on outboard sections due to three-dimensional effects. This shows the importance of calculating the noise metric, especially at high lift coefficients, with a characteristic velocity and length scale that vary along the span.

Acknowledgment

This work was supported by NASA Langley Research Center grant NAG 1-02024.

References

[1] Crighton, D. G., "Airframe Noise," *Aeroacoustics of Flight Vehicles: Theory and Practice, Volume 1: Noise Control*, edited by H. H. Hubbard, NASA World Radiation Data Center, TR 90-3052, 1991, pp. 397–447, Chap. 7.

[2] Lilley, G. M., "The Prediction of Airframe Noise and Comparison with Experiment," *Journal of Sound and Vibration*, Vol. 239, No. 4, 2001, pp. 849–859. doi:10.1006/jsvi.2000.3219

[3] Lockard, D. P., and Lilley, G. M., "The Airframe Noise Reduction Challenge," NASA Langley Research Center TM-2004-213013, Hampton, VA, April 2004.

[4] Goldstein, M. E., *Aeroacoustics*, McGraw–Hill, New York, 1976.

[5] Lilley, G. M., "A Study of the Silent Flight of the Owl," AIAA Paper 1998-2340, 1998.

[6] Howe, M. S., "A Review of the Theory of Trailing Edge Noise," *Journal of Sound and Vibration*, Vol. 61, No. 3, 1978, pp. 437–465. doi:10.1016/0022-460X(78)90391-7

[7] Lighthill, M. J., "On Sound Generated Aerodynamically. II. Turbulence as a Source of Sound," *Proceedings of the Royal Society of London A*, Vol. 222, 1954, pp. 1–32. doi:10.1098/rspa.1954.0049

[8] Ffowcs Williams, J. E., and Hall, L. H., "Aerodynamic Sound Generation by Turbulent Flow in the Vicinity of a Scattering Half Plane," *Journal of Fluid Mechanics*, Vol. 40, No. 4, March 1970, pp. 657–670. doi:10.1017/S0022112070000368

[9] Fink, M. R., *Airframe Noise Prediction Method*, Federal Aviation Administration, Rept. FAA-RD-77-29, March 1977.

[10] Brooks, T. F., Pope, S. D., and Marcolini, M. A., "Airfoil Self-Noise and Prediction," NASA Langley Research Center, Ref. Publ. 1218, Hampton, VA, July 1989.

[11] Zorumski, W. E., "Aircraft Noise Prediction Program Theoretical Manual," NASA Langley Research Center TM 83199, Hampton, VA, Feb. 1982.
[12] Singer, B. A., Brentner, K. S., Lockard, D. P., and Lilley, G. M., "Simulation of Acoustic Scattering from a Trailing Edge," AIAA Paper 1999-0231, 1999.
[13] Howe, M. S., *Acoustics of Fluid-Structure Interactions*, Cambridge Univ. Press, New York, 1998.
[14] GASP Reference Guide, Ver. 4.2, AeroSoft, Inc., Blacksburg, VA, 2004.
[15] Menter, F., "Two-Equation Eddy-Viscosity Turbulence Models for Engineering Applications," *AIAA Journal*, Vol. 32, 1994, pp. 1598–1605. doi:10.2514/3.12149
[16] Bardina, J. E., Huang, P. G., and Coakley, T. J., "Turbulence Modeling Validation," AIAA Paper 1997-2121, 1997.
[17] Harris, C., "NASA Supercritical Airfoils: A Matrix of Family Related Airfoils," NASA Langley Research Center TP 2969, 1990.
[18] Hosder, S., "Clean Wing Airframe Noise Modeling for Multi-disciplinary Design and Optimization," Ph.D. Thesis, Dept. of Aerospace and Ocean Engineering, Virginia Polytechnic Inst. and State Univ., Blacksburg, VA, July 2004; also http://scholar.lib.vt.edu/theses/available/etd-09072004-093109/ [retrieved 2 April 2010].
[19] Jacobs, P. F., and Gloss, B. B., "Longitudinal Aerodynamic Characteristics of a Subsonic, Energy-Efficient Transport Configuration in the National Transonic Facility," NASA Langley Research Center TP 2922, 1989.